Effects of global boundary and local collisionality on magnetic reconnection in a laboratory plasma

A. Kuritsyn,[1,2] H. Ji,[1] S. P. Gerhardt,[1] Y. Ren,[1] and M. Yamada[1]

Received 30 May 2007; revised 4 July 2007; accepted 24 July 2007; published 25 August 2007.

[1] The magnetic reconnection process is studied in a wide range of operating conditions in the well-controlled Magnetic Reconnection Experiment. The reconnection rate is observed to be a function of both global (system size) and local (collisionality) plasma parameters. When only local collisionality is lowered, the current sheet is shortened while effective resistivity is enhanced, both accelerating reconnection rates. At a fixed collisionality, the current sheet length increases with system size, resulting in the reduction of the reconnection rate. These results quantitatively agree with a generalized Sweet-Parker analysis. **Citation:** Kuritsyn, A., H. Ji, S. P. Gerhardt, Y. Ren, and M. Yamada (2007), Effects of global boundary and local collisionality on magnetic reconnection in a laboratory plasma, *Geophys. Res. Lett.*, *34*, L16106, doi:10.1029/2007GL030796.

1. Introduction

[2] Magnetic reconnection, a fundamental process in plasma physics, is the topological change of a magnetic field configuration in a highly conducting plasma through breaking and rejoining of magnetic field lines [*Biskamp*, 2000]. This process occurs in both space and laboratory plasmas and is considered to be the most likely mechanism for efficient conversion of magnetic field energy into plasma thermal and kinetic energy. In the classical Sweet-Parker model based on resistive magnetohydrodynamics (MHD) and Spitzer resistivity η_{Spitzer} [*Sweet*, 1958; *Parker*, 1957], the reconnecting current sheet is approximated by a rectangle with thickness δ and length L, the latter of which is assumed to be the system size. The predicted reconnection rate scales as $V_R/V_A = \delta/L = 1/\sqrt{S}$, where V_R is the reconnection inflow speed, Alfvén speed $V_A \equiv B/\sqrt{\mu_0 \rho}$ (here B is the reconnecting field and ρ is the mass density), and the Lundquist number S is defined as $\mu_0 L V_A/\eta_{\mathrm{Spitzer}}$. Since S is extremely large in space plasmas, this prediction gives rates too slow to be consistent with observations. The main reason for the small predicted rate is that the small resistivity causes the magnetic field to dissipate only in a very thin (microscopic δ) and very long (macroscopic L) current sheets, which impede the mass outflow and thus limit the reconnection rate. This problem thus exemplifies coupling between local dynamics and global boundaries.

[3] In order to accelerate the reconnection rate, two generally separate approaches have been taken: either to introduce [*Ugai and Tsuda*, 1977; *Hayashi and Sato*, 1978; *Kulsrud*, 1998] an anomalously large resistivity (compared to the Spitzer value) enhanced, for example, via wave-particle interactions, or alternatively, to shorten the current sheet length L. *Petschek* [1964] proposed that L can be made shorter than the system size by introducing standing shocks to open up the current sheet in the downstream region, allowing for faster mass outflow. However, it was later shown that such a current sheet structure is not compatible with uniform resistivity. By introducing effects beyond resistive MHD, especially the Hall effect, Petschek-like solutions have been re-established, opening up the downstream region in a laminar fashion [*Birn et al.*, 2001]. In the case of reconnection without an appreciable guide magnetic field, the Hall effect becomes important when δ becomes comparable to the ion skin depth, c/ω_{pi} (ω_{pi} is the ion plasma frequency). When ions enter the reconnection layer, they become unmagnetized and thus free to turn downstream, where they join electrons flowing out of the reconnection region. Therefore, the Hall effect limits δ to $\sim c/\omega_{pi}$. Then, a central question is how L is determined since the aspect ratio, δ/L, decides the reconnection rate in steady state. On the one hand, it was numerically shown [*Shay et al.*, 1999; *Huba and Rudakov*, 2004; *Sullivan et al.*, 2005] that L is limited to $\sim 10\delta \sim 10c/\omega_{pi}$ resulting in a universal reconnection rate of ~ 0.1, which is determined only by the local physics and is independent of the system size. On the other hand, several other analytic and numerical investigations [*Wang et al.*, 2001; *Fitzpatrick*, 2004; *Bhattacharjee et al.*, 2005] showed that the reconnection rate is not a universal constant, but rather depends on the system size. More recent full particle simulations using open boundary conditions [*Daughton et al.*, 2006; *Fujimoto*, 2006] showed that the current sheet extends towards the downstream boundary, resulting in substantially slower reconnection rates. Experimentally and observationally, however, there exist no systematic studies on how the current sheet length is related to the resistivity enhancement, as well as to the global system size, in determining the reconnection rate.

[4] In this Letter, we show, based on a well-controlled and diagnosed laboratory experiment (MRX), that the current sheet length and resistivity enhancement are not independently determined, as have been traditionally assumed, but rather are closely related in a self-consistent manner. At a given system size, the current sheet is shortened and the resistivity is enhanced with decreasing local collisionality, leading to faster reconnection. At a given resistivity, either classical or enhanced, the current sheet is lengthened as the global system size is increased,

[1]Center for Magnetic Self-Organization in Laboratory and Astrophysical Plasmas, Princeton Plasma Physics Laboratory, Princeton, New Jersey, USA.

[2]Center for Magnetic Self-Organization in Laboratory and Astrophysical Plasmas, Department of Physics, University of Wisconsin–Madison, Madison, Wisconsin, USA.

Copyright 2007 by the American Geophysical Union.
0094-8276/07/2007GL030796$05.00

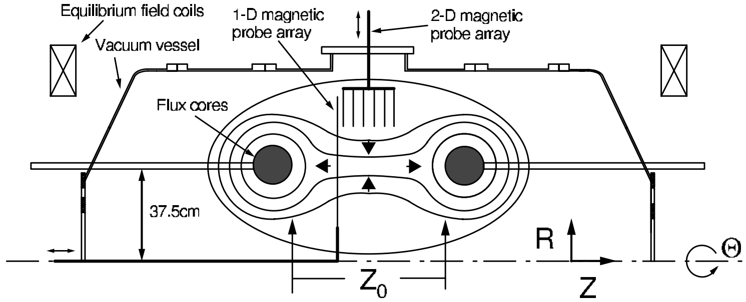

Figure 1. Schematic of the MRX apparatus.

resulting in slower reconnection. As a result, reconnection is found to be a process closely coupling local collisionality and the global boundary.

2. Apparatus and Methods

[5] The MRX [*Yamada et al.*, 1997] uses two flux-cores to create plasma and drive reconnection (Figure 1). Each flux-core has toroidal field (TF) and poloidal field (PF) coil windings. First, an "X-point" like magnetic configuration is established by parallel currents in the PF coils. Then, the currents in the TF coils are pulsed, creating an inductive electric field around the flux-cores to break down the gas. As the PF field currents are ramped down, the poloidal flux is pulled back towards the flux-cores. This induces a toroidal electric field at the X-point, driving axisymmetrical current along the toroidal (θ) direction. The separation between the flux-cores (Z_0) can be varied from 35 cm to 80 cm and serves as a measure of the system size. At a given Z_0, the TF and PF coil currents (with an approximately fixed ratio between them) and the fill pressure of the working gas (deuterium in the present experiments) can be varied. Experiments were done in a configuration without a guide field.

[6] The reconnection process in MRX is diagnosed by an extensive set of internal pick-up coils, which allow mapping of the magnetic field and calculation of the poloidal flux assuming axisymmetry: $\psi(R, Z, t) = \int_0^R 2\pi R' B_Z(R', Z, t) dR'$. The toroidal electric field is determined by $E_\theta = -(\partial\psi/\partial t)/2\pi R$. The radial profile of the reconnecting magnetic field, measured by a linear array of pick-up coils with 0.5 cm resolution, is fit well by a hyperbolic tangent function [*Yamada et al.*, 2000]. The current density profile is calculated as a derivative of the hyperbolic tangent fit: $\mu_0 j_\theta \approx -\partial B_Z/\partial R$. The current sheet half thickness, δ_{fit}, is also determined from the fit. An effective resistivity is defined as $\eta \equiv E_\theta/j_\theta$, and can be regarded as a measure of dissipation around the current sheet center. It has been found previously that η is much larger [*Ji et al.*, 1998; *Trintchouk et al.*, 2003; *Kuritsyn et al.*, 2006] than the classical perpendicular Spitzer resistivity at low collisionality, defined as the ratio of the current sheet thickness to the electron mean free path, δ/λ_{mfp}. The mechanism(s) for the resistivity enhancement by non-MHD effects is currently under investigation [*Ji et al.*, 2004; *Ren et al.*, 2005; *Yamada et al.*, 2006]. Plasma density n and electron temperature T_e are measured by a triple Langmuir probe and the flow speeds are determined by a Mach probe and by an optical probe. The typical plasma parameters are: $n \simeq (0.1–2) \times 10^{14}$ cm^{-3}, $T_e \simeq (3–15)$ eV, $B < 0.5$ kG.

[7] In order to study the interplay between local dynamics and global boundaries, the shape of the current sheet is approximated by a rectangular box with a half width δ and a half length L. At high collisionality, this approximation is quite accurate since the reconnection process is described well by the classical Sweet-Parker model [*Ji et al.*, 1998]. At low collisionalities, the reconnecting field lines change to a double wedge shape of Petschek type as the Hall effect becomes important [*Yamada et al.*, 2006]. Nevertheless, the contours of current density, j_θ, are still reasonably well approximated by a rectangular box, as shown in Figure 2. Since j_θ is dominated by $\partial B_Z/\partial R$, the decrease in j_θ at the current sheet edge is well characterized by an increase in the fitting parameter $\delta_{fit}(Z)$ for the measured $B_Z(R)$ with increasing $|Z|$. Thus, the current sheet length determined at the 50% level of the peak current density agrees well with the definition of L from the locations where δ_{fit} increases by a factor of 2 from its thinnest value (Figure 2). The latter method is used here because of its convenience. The current sheet half width, δ, is then determined by averaging δ_{fit} within the current sheet.

3. Anticorrelation Between Effective Resistivity and Current Sheet Length

[8] A first set of experiments was carried out by varying the fill pressure at a constant flux-core spacing and coil currents. Figure 3 shows key physical quantities versus inverse plasma collisionality. When the fill pressure, and thus the collisionality, is reduced, the effective resistivity η becomes larger than the Spitzer value, while the current sheet becomes shorter. This provides strong evidence that L is not simply set by the system size, as assumed in the classical Sweet-Parker model, but rather is collisionality dependent. Therefore, the resistivity enhancement and current sheet shortening are closely coupled in MRX, in sharp contrast to traditional theories. We note that the anti-correlation between η and L is also observed when coil currents are varied at fixed fill pressure.

[9] Qualitatively, the anti-correlation between η and L can be understood as follows. The plasma is accelerated downstream primarily by the magnetic tension force, which acts against increasing magnetic and thermal pressures. The current sheet length is determined by the balance between the tension force and the downstream pressures. Lowering the collisionality substantially reduces the neutral sheet

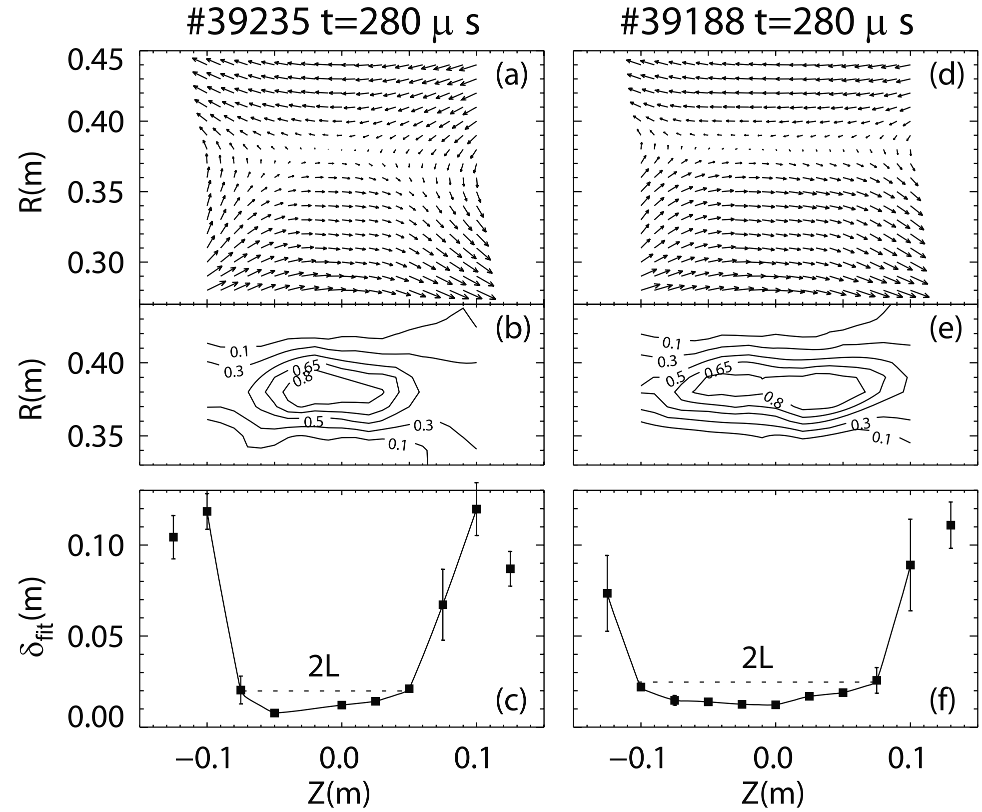

Figure 2. Examples of ((a) and (d)) magnetic field vector plots and ((b) and (e)) contours of current density normalized by its peak values at low (p_{fill} = 4.6 mT) and high (p_{fill} = 10.7 mT) collisionalities at Z_0 = 35 cm. ((c) and (f)) Also shown are δ_{fit} as functions of Z. The current sheet lengths determined from the broadening of δ_{fit} are consistent with those from current density contours. They are 6.2 cm and 9.0 cm, respectively.

current, due to the enhanced resistivity, while the downstream pressures remain roughly unchanged. This results in a smaller tension force, which can be balanced by the downstream pressures at a shorter distance from the X-line, and therefore a shorter current sheet forms. In a limiting case, when η approaches zero disallowing reconnection, L is maximized to the system size. In the opposite limit, when η approaches infinity, the neutral sheet current diminishes (as in a vacuum) with L approaching zero.

[10] Quantitatively, the anti-correlation between η and L is realized in such a way that their product, ηL, tends to be a constant, as shown in Figure 3c. This relation is supported by the following analysis based on the induction and continuity equations in (quasi) steady state:

$$V_R = \eta/(\mu_0 \delta), \qquad n_{up} V_R L = n_{down} V_Z \delta, \tag{1}$$

where V_R (V_Z) is the inflow speed into (outflow speed from) the diffusion region while n_{up} (n_{down}) is the density at the upstream (downstream). In the conventional Sweet-Parker analysis, V_R and δ are treated as unknowns while L is set to be the system size. When non-MHD effects become dominant, δ is largely limited by the ion skin depth [δ = (0.2–0.4)c/ω_{pi} in MRX], and thus cannot be regarded as an unknown. Instead, L is forced to vary, deviating from the system size. Solving for L by eliminating V_R from the above equations yields $\eta L = \mu_0 V_Z \delta^2$ (n_{down}/n_{up}). The RHS (open squares in Figure 3c), evaluated by independent measurements, stays approximately constant, in agreement with the LHS. As a result, the reconnection rate is accelerated not only by the resistivity enhancement but also by the current sheet shortening: $V_R \propto \sqrt{\eta/L}$. This is illustrated in Figure 3d where the measured reconnection rate increases substantially with decreasing collisionality.

4. Dependence on System Size

[11] While the product ηL is roughly constant and independent of the collisionality at a fixed flux-core spacing, it does change when the flux-core spacing is varied. At a fixed value of the resistivity anomaly factor $\eta/\eta_\perp^{Spitzer}$, the current sheet length L, and thus the product ηL (Figure 4a), increase with increasing flux-core spacing. This clearly demonstrates that L depends not only on the local collisionality, but also on the global system size. Since a longer L implies a slower reconnection rate at a given resistivity, the experimentally determined reconnection rate decreases with an increase of the flux-core spacing in both classical ($\eta \simeq \eta_\perp^{Spitzer}$) and anomalous ($\eta \simeq 3 \times \eta_\perp^{Spitzer}$) regimes as shown in Figure 4c.

[12] To better quantify the dependence of the reconnection rate on the system size, we employ a generalized Sweet-Parker analysis [*Ji et al.*, 1998, 1999] with some refinements. In addition to equation (1), the equations of motion relate the outflow speed V_Z to V_A, which is based on the reconnecting magnetic field and central density. The combined effects of the high downstream pressure and the plasma viscosity lead to the reduction of the outflow speed

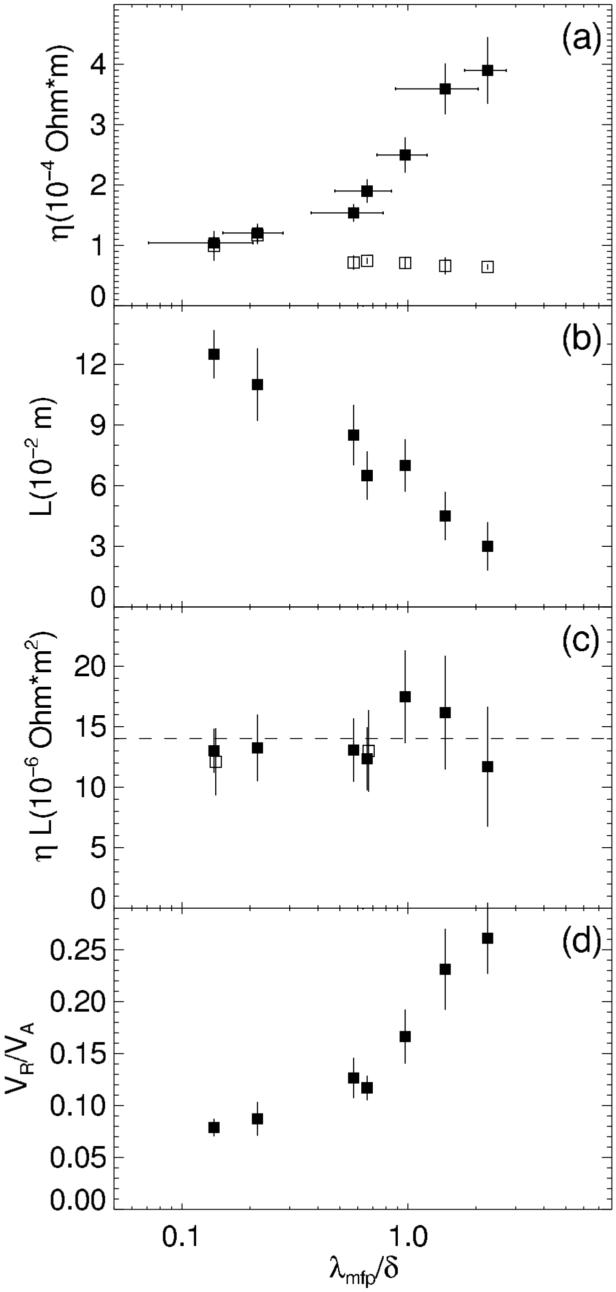

Figure 3. (a) Effective resistivity (filled squares) along with the Spitzer resistivity (open squares), (b) current sheet length, (c) product of the effective resistivity and the current sheet length (filled squares) and prediction of the generalized Sweet-Parker model (open squares), and (d) reconnection rate V_R/V_A versus inverse collisionality λ_{mfp}/δ at Z_0 = 50 cm.

to sub-Alfvénic levels of $0.1-0.2 V_A$ [*Ji et al.*, 1999; *Kuritsyn*, 2005] and thus limit the reconnection rate. In steady state, the reconnection rate then can be expressed as: $V_R/V_A = 1/\sqrt{S_{eff}}$, where

$$S_{eff} = (\mu_0 L V_A/\eta)(n_{up}/n_{down})(V_A/V_Z). \quad (2)$$

[13] The first factor on the RHS of equation (2) resembles the Lundquist number, where the Spitzer resistivity, however, is replaced by the experimentally determined effective resistivity and L is the measured current sheet length rather than the system size. The next factor represents the effect of the peaked density profile, and the last factor takes into account the measured sub-Alfvénic outflows.

[14] At a given resistivity, increasing the distance between the flux-cores allows more room not only to form a longer current sheet (Figure 4a), but also to expand the plasma to a lower density in the downstream region compared to the upstream. These lead to faster outflows, V_Z, as shown in Figure 4b, due to the reduced downstream pressure and viscous force. Therefore, when Z_0 is increased, the increase in the second factor of S_{eff} approximately cancels the decrease in the last term. Thus, the increase in S_{eff} is

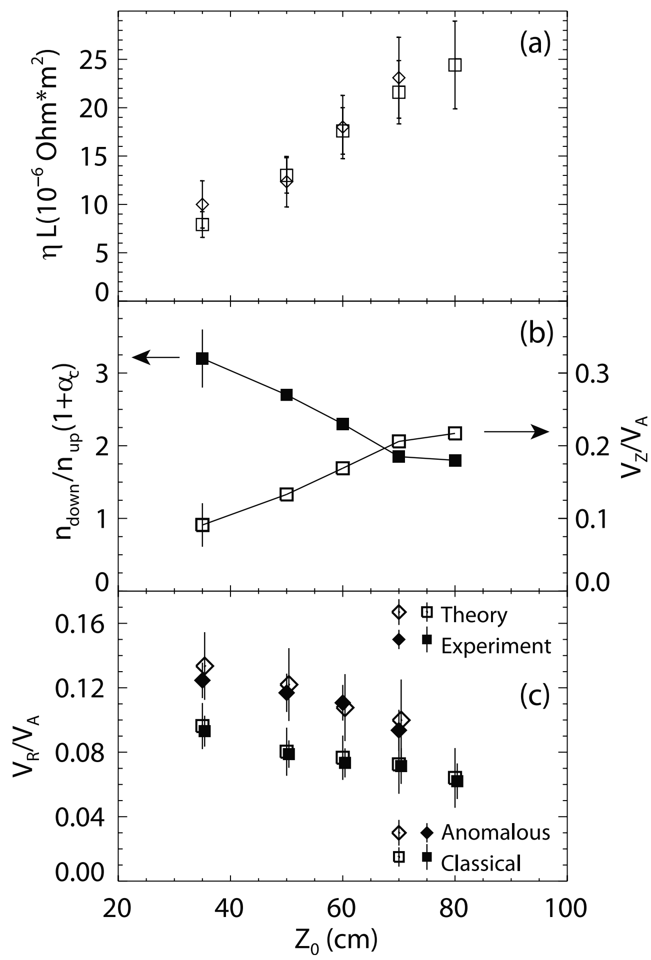

Figure 4. (a) Product of the effective resistivity and the current sheet length versus flux-core spacing in classical resistive MHD ($\eta \simeq \eta_\perp^{\rm Spitzer}$) (squares) and low-collisionality anomalous ($\eta \simeq 3 \times \eta_\perp^{\rm Spitzer}$) (diamonds) regimes. (b) Ratio of the downstream density to the upstream density (here $\alpha_c \equiv L\dot{n}_c/n_{down}V_Z$; n_c being central density) and normalized outflow speed in the classical regime. (c) Measured reconnection rate (filled symbols) and prediction of the generalized Sweet-Parker model (open symbols) for anomalous (top row of diamonds) and classical (bottom row of squares) regimes versus flux-core spacing.

dominated by the increase in L, leading to slower reconnection (Figure 4c).

5. Conclusions

[15] In summary, it is shown for the first time in a laboratory plasma that the reconnection rate is determined generally as a result of an interplay between collisionality-dependent local dynamics and global boundary conditions. At a given system size, the current sheet is shortened and the effective resistivity is enhanced when the collisionality is lowered. This can be understood as a consequence of the fact that the current sheet thickness is limited by the ion skin depth. We note that this is consistent with a trend generally observed in numerical simulations [e.g., *Daughton et al.*, 2006], although no explicit analysis has been given to our knowledge. When the system size is increased at a fixed collisionality, the current sheet length increases, resulting in slower reconnection. This is in contrast with the numerical results showing that the reconnection rate is independent of the system size [e.g., *Shay et al.*, 1999], while it is consistent with studies where the current sheet length depends on the system size [e.g., *Wang et al.*, 2001]. Since the system size was varied by only about a factor of 2 in the present study, further insights into this problem await experiments encompassing a wider parameter range as well as high resolution numerical simulations with proper boundary conditions.

[16] **Acknowledgments.** The authors thank R. Kulsrud, J. Drake, X. Wang, W. Daughton, and A. Bhattacharjee for stimulating comments. This work is supported by U.S. DOE, NASA, and NSF.

References

Bhattacharjee, A., K. Germaschewski, and C. S. Ng (2005), Current singularities: Drivers of impulsive reconnection, *Phys. Plasmas*, *12*, 042305.
Birn, J., et al. (2001), Geospace environmental modeling (GEM) magnetic reconnection challenge, *J. Geophys. Res.*, *106*, 3715.
Biskamp, D. (2000), *Magnetic Reconnection in Plasmas*, Cambridge Univ. Press, Cambridge, UK.
Daughton, W., J. Scudder, and H. Karimabadi (2006), Fully kinetic simulations of undriven magnetic reconnection with open boundary conditions, *Phys. Plasmas*, *13*, 072101.
Fitzpatrick, R. (2004), Scaling of forced magnetic reconnection in the Hall-magnetohydrodynamic Taylor problem, *Phys. Plasmas*, *11*, 937.
Fujimoto, K. (2006), Time evolution of the electron diffusion region and the reconnection rate in fully kinetic and large system, *Phys. Plasmas*, *13*, 072904.
Hayashi, T., and T. Sato (1978), Magnetic reconnection: Acceleration, heating, and shock formation, *J. Geophys. Res.*, *83*, 217.
Huba, J., and L. Rudakov (2004), Hall magnetic reconnection rate, *Phys. Rev. Lett.*, *93*, 175003.
Ji, H., M. Yamada, S. Hsu, and R. Kulsrud (1998), Experimental test of Sweet-Parker model of magnetic reconnection, *Phys. Rev. Lett.*, *80*, 3256.
Ji, H., M. Yamada, S. Hsu, R. Kulsrud, T. Carter, and S. Zaharia (1999), Magnetic reconnection with Sweet-Parker characteristics in two dimensional laboratory plasmas, *Phys. Plasmas*, *6*, 1743.
Ji, H., S. Terry, M. Yamada, R. Kulsrud, A. Kuritsyn, and Y. Ren (2004), Electromagnetic fluctuations during fast reconnection in a laboratory plasma, *Phys. Rev. Lett.*, *92*, 115001.
Kulsrud, R. M. (1998), Magnetic reconnection in a magnetohydrodynamic plasma, *Phys. Plasmas*, *5*, 1599.
Kuritsyn, A. (2005), Experimental study of the effects of boundary conditions and guide field on magnetic reconnection, Ph.D. thesis, Princeton Univ., Princeton, N. J.
Kuritsyn, A., M. Yamada, S. Gerhardt, H. Ji, R. Kulsrud, and Y. Ren (2006), Measurements of the parallel and transverse Spitzer resistivities during collisional magnetic reconnection, *Phys. Plasmas*, *13*, 055703.
Parker, E. N. (1957), Sweet's mechanism for merging magnetic fields in conducting fluids, *J. Geophys. Res.*, *62*, 509.
Petschek, H. E. (1964), *AAS-NASA Symposium on Solar Flares* (*National Aeronautics and Space Administration, Washington, DC*), *NASA Spec. Publ.*, *SP-50*, 425 pp.
Ren, Y., M. Yamada, S. Gerhardt, H. Ji, R. Kulsrud, and A. Kuritsyn (2005), Experimental verification of the Hall effect during magnetic reconnection in a laboratory plasma, *Phys. Rev. Lett.*, *95*, 055003.
Shay, M. A., J. F. Drake, and B. N. Rogers (1999), The scaling of collisionless, magnetic reconnection for large systems, *Geophys. Res. Lett.*, *26*, 2163.
Sullivan, B. P., B. N. Rogers, and M. A. Shay (2005), The scaling of forced collisionless reconnection, *Phys. Plasmas*, *12*, 122312.
Sweet, P. A. (1958), The neutral point theory of solar flares, in *Electromagnetic Phenomena in Cosmical Physics*, p. 123, Cambridge Univ. Press, New York.
Trintchouk, F., M. Yamada, H. Ji, R. M. Kulsrud, and T. A. Carter (2003), Measurement of the transverse Spitzer resistivity during collisional magnetic reconnection, *Phys. Plasmas*, *10*, 319.
Ugai, M., and T. Tsuda (1977), Magnetic field-line reconnection by localized enhancement of reconnection. 1. Evolution in a compressible MHD fluid, *J. Plasma Phys.*, *17*, 337.
Wang, X., A. Bhattacharjee, and Z. W. Ma (2001), Scaling of collisionless forced reconnection, *Phys. Rev. Lett.*, *87*, 265003.
Yamada, M., H. Ji, S. Hsu, T. Carter, R. Kulsrud, N. Bretz, F. Jobes, Y. Ono, and F. Perkins (1997), Study of driven magnetic reconnection in a laboratory plasma, *Phys. Plasmas*, *4*, 1936.
Yamada, M., H. Ji, S. Hsu, T. Carter, R. Kulsrud, and F. Trintchouk (2000), Experimental investigation of the neutral sheet profile during magnetic reconnection, *Phys. Plasmas*, *7*, 1781.
Yamada, M., Y. Ren, H. Ji, J. Breslau, S. Gerhardt, R. Kulsrud, and A. Kuritsyn (2006), Experimental study of two-fluid effects on magnetic reconnection in laboratory plasma with variable collisionality, *Phys. Plasmas*, *13*, 052,119.

S. P. Gerhardt, H. Ji, A. Kuritsyn, Y. Ren, and M. Yamada, Center for Magnetic Self-Organization in Laboratory and Astrophysical Plasmas, Princeton Plasma Physics Laboratory, P.O. Box 451, Princeton, NJ 08543, USA. (hji@pppl.gov)